REPRODUCTIVE BIOLOGY: ORIGINAL ARTICLE

miR-149-PARP-2 Signaling Regulates E-cadherin and N-cadherin Expression in the Murine Model of Endometrium Receptivity

Raj Kumar Verma[1] · Upendra Kumar Soni[1] · Sangappa Basanna Chadchan[1] · Vineet Kumar Maurya[1] · Mohini Soni[2] · Sudarsan Sarkar[1,3] · J. Venkatesh Pratap[2,3] · Rajesh Kumar Jha[1,3]

Abstract
Cadherins play an essential role in the attachment of the blastocyst to the endometrium, a process known as endometrial receptivity. Loss of E-cadherin expression is essential during the process, while the expression level of the other cadherin, N-cadherin, has been reported to be altered in cases of infertility. Both E-cadherin and N-cadherin can be regulated by members of the PARP family. Specifically, PARP-2, which is under the epigenetic control of miR-149, has been observed to promote E-cadherin expression in other human cells. We investigated the roles of E-cadherin and N-cadherin in endometrial receptivity using mouse models for normal endometrial receptivity, pseudopregnancy, and LPS-induced endometrial receptivity failure. E-cadherin and phosphorylated E-cadherin were predominantly expressed during pre-receptive stages as well as in the implantation site of the receptive stage, which were observed reduced during the later stages of implantation in both implantation and non-implantation regions, while N-cadherin was detected only at pre-receptive stages. E-cadherin and N-cadherin were also seen in the uterus during pseudopregnancy, showing a downregulation trend during receptive and post-receptive stages. LPS-induced failed endometrial receptivity showed upregulation of E-cadherin and downregulation of N-cadherin. The E-cadherin expression promoter, GSK-3, was lost and its suppressor, SLUG was upregulated during normal course of endometrial receptivity in mouse model, while GSK-3 was increased during LPS-induced failed embryo implantation. In an in vitro model of embryo implantation, E-cadherin expression is promoted by PARP-2 and regulated by miR-149 epigenetically in human endometrium epithelial cells. In conclusion, E-cadherin is predominantly expressed during pre-receptive stage and promoted by PARP-2, which is regulated by miR-149 in the endometrial epithelial cells.

Keywords E-cadherin · N-cadherin · SLUG · Glycogen synthase kinase (GSK)-3 · MicroRNA (miR)-149 · Poly(ADP-ribose) polymerase-2 (PARP-2) · Caspase-8 · Endometrial receptivity · Pseudopregnancy · Endometrial receptivity failure

Raj Kumar Verma, Upendra Kumar Soni and Sangappa Basanna Chadchan contributed equally to this work.

✉ Rajesh Kumar Jha
rajesh_jha@cdri.res.in

Raj Kumar Verma
rjverma7860@gmail.com

Upendra Kumar Soni
upendrasoni20@gmail.com

Sangappa Basanna Chadchan
sangam02@gmail.com

Vineet Kumar Maurya
mauryavineet.28@gmail.com

Mohini Soni
mohinisoni2017@gmail.com

Sudarsan Sarkar
sudarsansarkar93@gmail.com

J. Venkatesh Pratap
jvpratap@cdri.res.in

1 Female Reproductive Biology Laboratory, Division of Endocrinology, CSIR-Central Drug Research Institute, Sector-10, Jankipuram Extension, Sitapur Road, Lucknow 226031, India

2 Biochemistry and Structural Biology Division, CSIR-Central Drug Research Institute, Sector-10, Jankipuram Extension, Sitapur Road, Lucknow 226031, India

3 Academy of Scientific and Innovative Research (AcSIR), Ghaziabad 201002, UP, India

Introduction

Endometrial receptivity is a narrow window of endometrium that facilitates competent blastocyst implantation. The endometrial receptivity is a highly ordered intricate and complex process. Implantation involves apposition, adhesion, and penetration, and several molecular pathways including cytokines, transcription factors, ovarian steroids, and adhesion molecules have been discovered that contribute to successful endometrial receptivity establishment. During endometrial receptivity, the blastocyst attaches with the help of adhesion molecules (integrins and cadherins) and forms an intricate relation with the mother tissue, endometrium to obtain support until birth. It has been shown that inadequate endometrial receptivity causes two-thirds of implantation failures [1] even in ovarian pathophysiological conditions [2]. E-cadherin has been identified to play a role in the endometrial receptivity for embryo implantation [3]. More specifically, it has been demonstrated that upregulation of of E-cadherin to human endometrial epithelial cells favors receptivity [4]. E-cadherin and N-cadherin have also been reported in the epithelial-mesenchymal transition (EMT) [5, 6], which takes place during the window of endometrial receptivity [7]. E-cadherin is epigenetically regulated in endometrial epithelial cells [4, 8]. These mechanisms of regulation contribute to the roles of E-cadherin in the adherens junctions, including maintenance of cell polarity and prevention of EMT. It has recently been shown that the cell polarity, through stabilizing adherens junction protein E-cadherin and preventing EMT, leads to non-receptive endometrium [9]. In fact, E-cadherin expression has been reported to be downregulated in pregnancy failure cases [10], while the other cadherin, N-cadherin, is altered in infertility cases [11].

Regulation of E-cadherin and N-cadherin has not been studied fully at the post-transcription level. Poly(ADP-ribose)polymerase, PARP-1, can regulate E-cadherin [12], and PARP-1 is already reported in the endometrial receptivity [13]. Another isoform form of PARP, PARP-2, has also recently been found crucial for the endometrial receptivity [14, 15]. Both PARP-2 and caspase-8 have recently been reported during endometrial receptivity events where PARP-2 expression is an essential promoter of implantation and caspase-8, a negative regulator of PARP-2, inhibits implantation [14, 15]. Expression level of PARP-2 was diminished while that of caspase-8 was increased during failed endometrial receptivity for blastocyst implantation [15, 16]. At the post-transcriptional level, *PARP-2* is regulated by miR-149, but whether caspase-8 is also regulated by miR-149 is still unknown [14, 16].

In the endometrial epithelial and stromal cells, miR-149 regulates PARP-2 expression and negatively affects the trophoblast attachment process [14]. We hypothesized that miR-149-mediated PARP-2 expression might regulate the expression of E-cadherin and N-cadherin during the endometrial receptivity. In the present investigation, we attempted to find the miR-149-PARP-2-mediated epigenetic regulation of E-cadherin and N-cadherin in the endometrium during its receptivity phases using mouse models and human endometrial epithelial cell line.

Materials and Methods

Mouse Model of Embryo Implantation

Healthy 12–13-week-old female mice *(Mus musculus,* Swiss strain) were used in this study. Animal handling and care was followed according to the Animal Ethical Committee Guidelines of Council of Scientific and Industrial Research (CSIR)-Central Drug Research Institute (CDRI), Lucknow, India, and this study was approved via application file nos. IAEC/2013/27 dated March 07, 2013 and IAEC/2019/39/ dated 04/01/2019. Pregnancy was established in the female mouse as described in our earlier reports [15, 17]. Implantation sites (IS) in the uterus were identified by tail vein injection of Evan's blue dye as distinct blue colored bands, while colorless or faint areas between the two implantation regions were considered as non-implantation sites (NIS) [15, 18]

Pseudopregnancy Mouse Model

Pseudopregnancy were established in the female mouse as described in our previous reports by caging two normal cycling females with the one vasectomized male [17]. The mating day was identified by presence of vaginal plug and considered as day 1. Implantation sites (IS) in the uterus were visualized by tail vein injection of Evan's blue dye [18]. Unlike normal pregnancy model, the pseudopregnant animals completely lack the IS due to pseudopregnancy.

LPS-Induced Endometrial Receptivity Failure Model

We recapitulated the lipopolysaccharide (LPS)-induced implantation failure model as published previously (Deb et al. 2004) [15]. Pregnant female mice were intra-peritoneally injected either LPS (L2654, Sigma-Aldrich, Bangalore, India) at 10 μg/25 gm body (b.) weight (wt.) or vehicle as control group on day 1 (1000 h) post-coitus (p.c.) Evan's blue dye was injected through the tail vein on day 5 (1000 h) p.c., and the IS and NIS were macro-photographed [15, 17]. The blastocysts were gently flushed out in sterile saline and observed on a phase contrast inverted microscope (CKX41 Trinocular and Q-Imaging MP5.0-RTV-CLR-10-C,

Olympus, Japan) to confirm the stage of pregnancy. Uterine tissues were either frozen or used for immunoblotting experiments.

hs-miR-149 Overexpression in Human Endometrial Epithelial Cells (hEECs)

The Ishikawa (endometrial adenocarcinoma) (hEECs) (ECACC cat no. 99040201) are acceptable model of endometrial epithelial cell for the in vitro embryo/trophoblast implantation-related studies as reported by other groups [19–22] and our group [14, 17, 23]. Therefore, we had followed the established cell lines in the present study. Ishikawa; hEECs (ECACC cat no. 99040201) was purchased Sigma-Aldrich Inc., Bangalore, India (ECACC) and maintained in the 10% FBS-supplemented MEM culture medium. The human-specific miR-149 plasmid vector (SC400186) and control vector (PCMVMIR) were purchased from OriGene Technologies, Inc., MD, USA, and were propagated in *E. coli* DH5α (New England Biolabs, MA, USA). Using Lipofectamine-2000 reagent (Invitrogen, Bangalore, India), the purified miR-149 plasmid vector or control vector was transfected in the hEECs according to the manufacturer's protocol and incubated for 48 h.

Co-culture of Human Trophoblast Cells (hTBLC) 3D Spheroids on a hEEC Monolayer for Attachment Assay

The co-culture of hTBLC 3D spheroids on a hEEC monolayer was performed according to the method described earlier [14, 17, 24]. The three-dimensional (3D) spheroids of hTBLCs were prepared by the hanging drop method, which were labeled with 10 μM Cell-Tracker orange dye (C34552, Invitrogen, Bangalore, India) [14]. First, the miR-149 overexpression was done by hEEC monolayers transfecting with either miR-149 plasmid or control vector for 48 h. The 3D spheroids were co-cultured with the hEEC monolayer, and the non-attached 3D spheroids were washed out with sterile PBS washing after 1-h incubation. The attached 3D spheroids were imaged after 24 h (expansion) using a microscope with a 20×objective lens (CKX41 Trinocular with Cooled CCD Camera Model Q Imaging MP5.0-RTV-CLR-10-C from Olympus, Tokyo, Japan).

PARP-2 and Caspase-8 Inhibition in hEECs

We inhibited PARP-2 and caspase-8 activities as described earlier [14]. hEECs at 70% confluency were treated with a selective PARP-2 activity inhibitor (UPF-1069, Sigma-Aldrich Inc., MO, USA) at a concentration of 0.3 μM and incubated for 24 h. The caspase-8 activity inhibitor was used at a concentration of 50 mM (sc-3083 Santa Cruz

Biotechnology, CA, USA), and incubated for 24 h at 37 °C and 5% CO_2 in humidified condition. The control was set for both PARP-2 and caspase-8 inhibition assay in the hEECs using the same concentration of DMSO as used in the respective drug concentration. After 24-h incubation, the protein was extracted from cells using RIPA buffer (20–188, Merck-Millipore, MA, USA,) and used for immunoblotting.

Immunohistochemistry

Immunostaining on the longitudinal uterine tissue sections (5.0 μm) was carried out as described previously [15, 17, 25]. The uterus was fixed in 4% paraformaldehyde at 4 °C for 1 h and dehydrated in ethanol gradient (50–90%), and xylene and paraffin-wax blocks were prepared. Uterine tissue sections were cut serially using microtome (Leica Biosystem, Wetzlar, Germany) and mounted on glass slides (coated with Vectabond reagent, Vector Laboratories, Inc., CA, USA). The paraffin-wax tissue sections were de-paraffinized in xylene overnight and rehydrated in ethanol gradient (90, 80, 70, and 50%) and water followed by antigen unmasking in 10 mM, pH 6.0 citrate buffer. The tissue sections were blocked in normal rabbit serum for 1 h. Anti-PARP-2 rabbit IgG (ab176330) or normal rabbit IgG (2729, Cell Signaling Technology, MA, USA) (isotype control) were used at 1:100 dilutions and incubated overnight at 4 °C. The tissue sections were incubated with biotinylated secondary antibody followed by ABC reagent (PK-4001, Vector Laboratories Inc.). Washing of PBS-T were given after each step. Signals were detected by chromogenic substrate of peroxidase (3,3′-diaminobenzidine tetrahydrochloride; DAB, Vector Laboratories Inc.) method and imaged under the microscope equipped with Cooled CCD Camera (CKX41 Trinocular and l Q Imaging MP5.0-RTV-CLR-10-C, Olympus, Japan).

Localization of E-cadherin in hEECs

We performed the immunolocalization of E-cadherin on hEECs grown on poly-l-lysine treated glass coverslips. Cells were fixed with 4% paraformaldehyde (prepared in PBS) for 15 min and permeabilized with 0.25% Triton X-100 for 10 min followed by blocking with 5% goat serum for 1 h. Cells were labeled for 2 h Alexa Fluor-568 tagged anti-E-cadherin primary antibody (Table 1) at 1:150 dilutions in 1% goat serum (diluted in PBS-T), for 2 h. Normal rabbit IgG was used as an isotype (negative) control for E-cadherin antibody specificity. The nucleus was counterstained with 4′,6-diamidino-2-phenylindole (DAPI) (0.5 μg/mL) for 5 min. The cells were washed three times with PBS after each incubation. Images were captured with a confocal laser scanning microscope (TCS SP5, Leica, Germany) at

63 × objective magnification and 3 × digital zoom (189 ×) in oil medium.

Protein Extract Preparation from the Uterus and Cells

Total protein extract from uterus and cells were prepared in 200 µl protein extraction buffer containing 100 mM KCL, 3 mM NaCl, 3.5 mM MgCl$_2$, 10 mM PIPES, phosphatase inhibitor (P5726, Sigma-Aldrich Inc., Bangalore, India), and protease inhibitor cocktail (S8830, Sigma-Aldrich Inc.) (pH 7.4) as described previously [13, 15, 24]. Uterine tissue was minced and homogenized followed by centrifugation at 200 × g for 10 min. The supernatant was centrifuged a second time at 1475 × g for 10 min at 4 °C, and the resultant supernatant was again centrifuged at 12,000 × g for 10 min.

Cells were directly homogenized in the RIPA buffer at 4 °C. The final uteri and cell supernatants, designated as crude cytosolic protein extract, were stored at − 80 °C in a Ultra-Low Temperature Freezer (U410, Eppendorf, NJ, USA) until use [15, 26].

SDS-PAGE Western Blotting and Immunoblotting

Tissue or cell protein lysates were separated by SDS-PAGE and electroblotted as described previously [15, 27]. The blotted membrane was incubated in 5% non-fat milk blocker (170–6404, Bio-Rad Laboratories India Pvt. Ltd., India) for 1 h at room temperature (RT). Blots were then incubated with corresponding primary antibodies (Table 1) in 2% non-fat milk for total proteins or 2% BSA for phosphorylated proteins overnight at 4 °C followed by incubation with suitable HRP-conjugated secondary antibodies in 1:3000 dilutions in 2% blocker for 1 h. After each incubation, three washings were done with TBS-T buffer (10 mM, pH 7.4 containing 0.1% Tween-20). Protein bands were visualized using ECL reagent (WBKLS0500, Merck-Millipore, Bangalore, India) and imaged using the Chemi-Imager/Documentation System (Image Quant LAS 4000, GE Life Science, PA, USA).

Transfection and Luciferase Assays

A transfection of hEECs and luciferase assays were performed as described previously [16]. Plasmid/vector were transfected to hEECs using Lipofectamine 2000 (11668027, Thermo Fisher Scientific, India) in 2 mL of Opti-MEM medium (31985070, Thermo Fisher Scientific, India) for 24 h in a 6-well culture plate. hEECs were either transfected alone or co-transfected with the following constructs; 2.5 µg of pMirTarget-3′UTR-PARP-2-luciferase reporter (SC200982, OriGene Technologies, Inc., MD, USA) with 5 µg of hs miR-149 (SC400186, OriGene, Technologies, Inc.) or 2.5 µg pMirTarget-control-luciferase reporter plasmid (PS100062 OriGene Technologies, Inc.) with 5 µg of hs miR-149 vector. The protein lysate was prepared in 200 µl of 1X luciferase cell lysis buffer (25 mM Tris–phosphate, 2 mM DTT, 2 mM trans-1,2, diaminocyclohexane-N,N,N', N tertaacetic acid, 10% glycerol, and 1% Triton X-100).

Table 1 List of the primary antibodies used for western blotting and immunolocalization (IHC and IF) assays

S. No	Antibody	Catalog No	Source	Dilution	References
A	**Application**		**Immunoblotting (IB)**		
1	Anti-mouse IgG Light chain specific	115–035-174	Jackson ImmunoResearch Lab. Inc., USA	1:3000	[35]
2	p-E-cadherin (phospho S838 + S840)	ab76319	Abcam, Cambridge, MA, USA	1:1000	[36]
3	Alexa Fluor® 555 Anti-E Cadherin antibody [EP700Y]	ab206878		1:1000	[14]
7	N-cadherin (Rabbit IgG)	14215S	Cell Signaling Technology Inc., MA, USA	1:1000	[37]
8	E-cadherin (Rabbit IgG)	3195S		1:1000	[14] [37]
9	SLUG (Rabbit IgG)	9585 S		1:1000	[38]
10	GSK3 (Rabbit IgG)	9315 S		1:1000	[39]
11	Normal rabbit IgG	2729		1:1000	[14] [40]
12	Anti-Rabbit IgG-HRP linked	7074S		1:3000	[14] [41]
13	Anti-rabbit HRP linked	A0545	Sigma-Aldrich Inc., Bangalore, India	1:3000	[17]
14	β-Actin	A3854		1:5000	[14, 42]
C	**Application**		**Immunofluorescence (IF) and IHC-Fr**		
1	Alexa Fluor® 555 Anti-E Cadherin antibody [EP700Y]	ab206878	Abcam, Cambridge, MA, USA	1:200	[14]
2	PARP-2	SAB2500757	Merck, Bangalore, India	1:200	[14]

Then, 50 µl of cell lysate was mixed with luciferase assay buffer (15 mM potassium phosphate pH 7.8, 25 mM glycyl-glycine, 15 mM MgSO4, 4 mM EGTA, and 2 mM ATP) and loaded in a 96-well culture plate with 100 µl of 2X Luciferin substrate (88,293, Thermo Fisher Scientific, India) in each well. The luminescence kinetics (up to 10 min) were immediately recorded by SpectraMax M2 (Molecular devices, LLC, USA), and the Luciferase activity was reported in terms of relative light unit (RLU).

Statistical Analysis

All in vivo experiments were performed with a minimum of three animals per group, and in vitro experiments were replicated independently three times. Band intensities from immunoblot were analyzed using TotalLab Quant 1D gel analysis software version 5.01 (Nonlinear Dynamics Ltd., Newcastle upon Tyne, UK). Respective replicate values were normalized to the corresponding β-actin (for cytosolic and whole cell lysate) values. The data from all experiments including Western blotting and fluorescence intensity analyses were plotted as mean with SEM. The data were subjected to Student's *t*-test through MS Excel 2016 for two group comparison, and more than two groups were analyzed using ANOVA followed by Tukeys test through Graph-Pad Prism 5.0 to calculate the significance among groups ($***p < 0.001$, $**p < 0.01$, $*p < 0.05$, NS $p > 0.05$).

Results

E-cadherin Expression Is Decreased in the Endometrium During Peri-implantation Stage

E-cadherin is present during pre-implantation stages (day 4,1000 h and 1600 h) in the endometrium of the mouse model for endometrial receptivity (Fig. 1A) and decreased during receptive stage (day 5, 0500 h) and remained low during next stage, post-receptive stage, day 5,1000 h. The implantation and non-implantation sites of day 5 (0500 h) and day 5 (1000 h) showed no difference, with the implantation site of day 5(0500 h) stage showing a higher expression level than the day 5 (1000 h) stage.

Likewise, the expression level of phosphorylated E-cadherin was seen high during pre-receptive (day 4, 1000 h), late-pre-receptive (day 4, 1600 h) and receptive stages (day 5, 0500 h), decreasing at the post-receptive stage (day 5, 1000 h) (Fig. 1B). At the receptive stage, the implantation site showed higher expression than the non-implantation site. Later, at day 5 (1000 h) stage, the expression levels of phosphorylated-E-cadherin was decreased in both implantation and non-implantation sites with the two regions showing similar levels (Fig. 1B).

Subsequently, we determined the expression level of E-cadherin during pseudopregnancy. E-cadherin was present throughout the stages of window of endometrial receptivity in pseudopregnancy. However, the expression level of E-cadherin was high in the endometrium from the pre-implantation stages (day 4, 1000 h and 1600 h) and decreased during subsequent stages (day 5, 0500 and 1000 h) during pseudopregnancy though, no statistically significant differences among the stages in the E-cadherin expression levels were observed (Fig. 1C).

Further, we recapitulated the lipopolysaccharide (LPS)-induced embryo implantation failure model (Fig. 1D) where the blastocyst and implantation sites were abolished at day 5(1000 h) by LPS treatment. We analyzed the expression level of E-cadherin, which was seen poorly expressed in the endometrium of control group's implantation site, but present in higher levels in the non-implantation site of day 5(1000 h) (Fig. 1E). E-cadherin was observed high in the LPS-induced endometrial receptivity failed group (Fig. 1E).

We evaluated the cellular distribution of the E-cadherin in the endometrium during the window of endometrial receptivity period and LPS-induced implantation failure mouse model (Fig. 2A and B). We observed the expression of E-cadherin in the epithelial (luminal and glandular) and stromal cells during the pre-receptive phase (day 4, 1000 h) and the subsequent stage, late-pre-receptive stage (day 4, 1600 h), (Fig. 2A). In the receptive stage (day 5, 0500 h) of endometrial receptivity, the expression of E-cadherin was predominantly seen in the endometrial stromal and luminal epithelial cells and mild in the glandular epithelial cells, while in the subsequent post-receptive stage (day 5, 1000 h), its expression was predominant in the stromal and myometrial cells, but mild in the epithelial cells (luminal and glandular) (Fig. 2A). The normal rabbit IgG immunolabelling to the uterine tissue did not show significant staining, suggesting the E-cadherin specific immunostaining (Fig. 2A).

The endometrial tissue of normal embryo implantation group without LPS treatment showed a strong immunoreactivity of E-cadherin in the stromal and luminal epithelial cells and weaker in the glandular epithelial cells at day 5 (1000 h p.c.). The expression of E-cadherin in the LPS-induced implantation failure model was not different than the LPS-treated group (Fig. 2B). We could not see the distinguished expression of E-cadherin in the implantation and non-implantation regions.

N-cadherin Expression Is Decreased in the Endometrium During Receptive stage

Likewise, the expression level of another cadherin, N-cadherin, was examined in the endometrium during the endometrial receptivity window (Fig. 3). N-cadherin is detected strongly during pre-receptive stage of endometrial
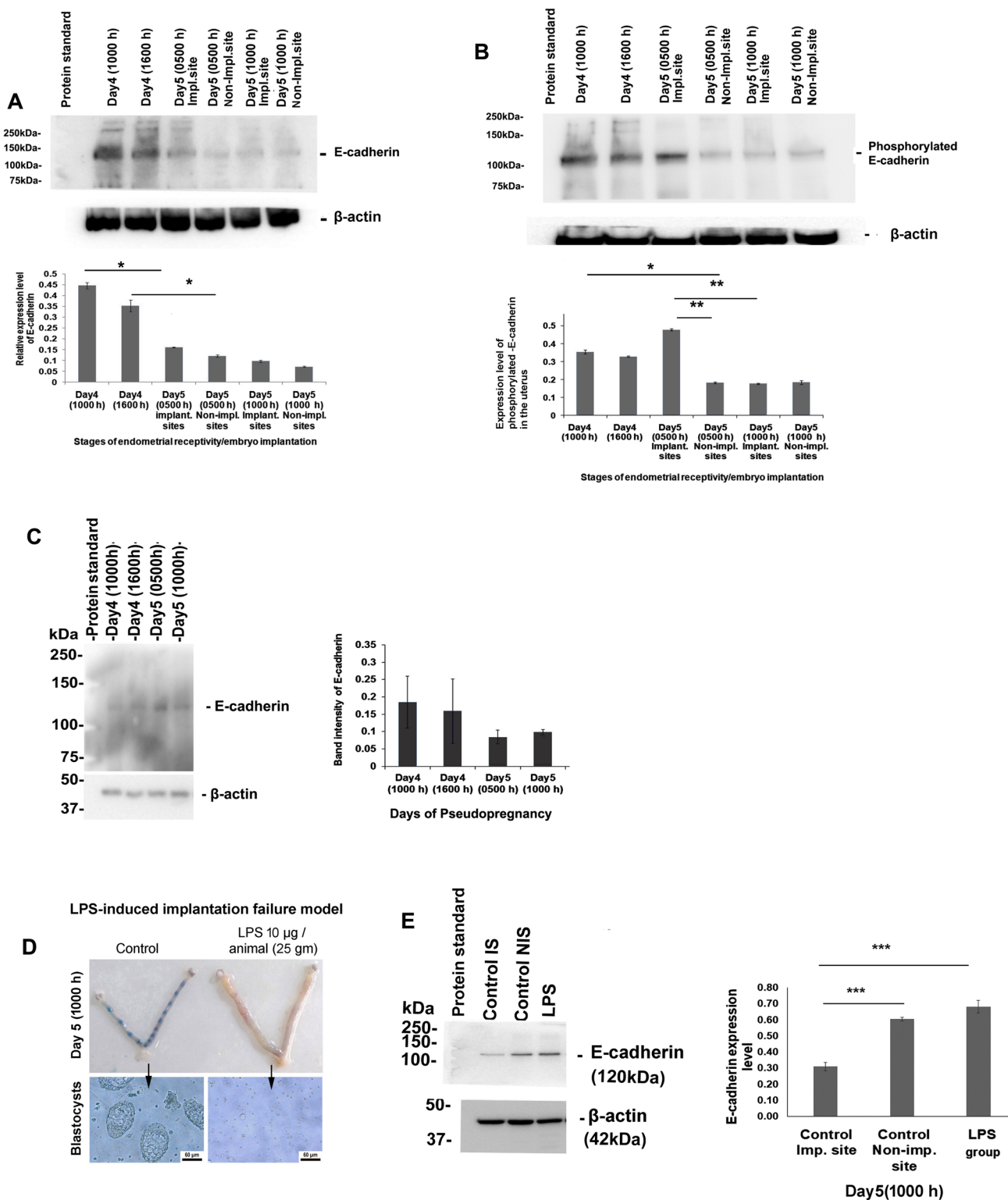
Fig. 1 E-cadherin and phosphorylated E-cadherin is differentially expressed in the endometrium during endometrial receptivity period in the mouse model. (A–B) Expression profiling of E-cadherin, and phosphorylated E-cadherin was done using immunoblotting and densitometric analysis in the mouse endometrium during window of receptivity for the blastocyst implantation. (C) During pseudo-pregnancy, E-cadherin expression pattern was analyzed in the endometrium. (D) Normal embryo implantation and LPS-induced failed embryo implantation was observed at day 5(1000 h) in the mouse model. (E) Expression analysis of E-cadherin was done in the endometrium from LPS-induced implantation failure mouse model. ($N = 3$) (**$p < 0.005$, *$p < 0.05$, NS $p > 0.05$)
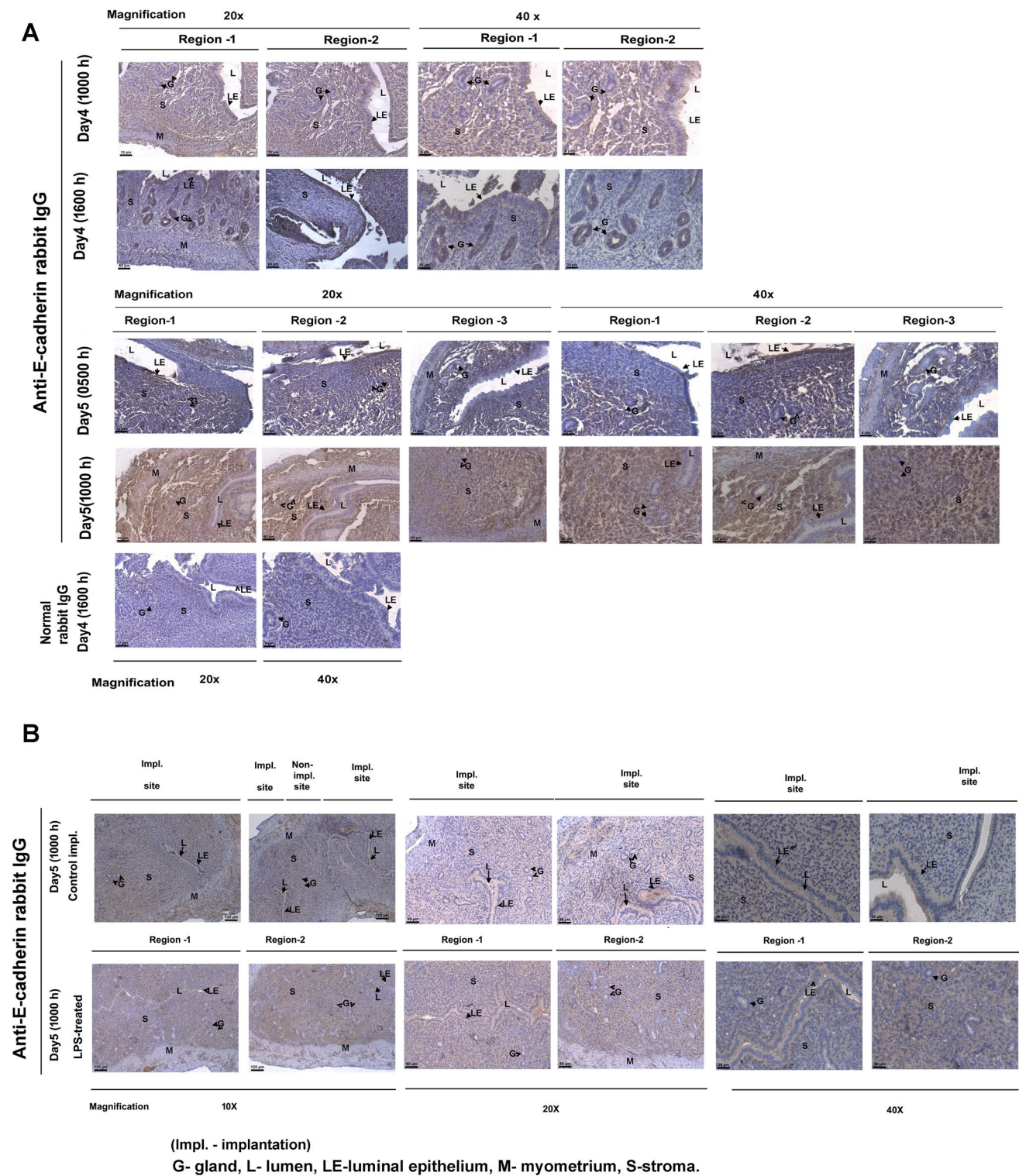
Fig. 2 Spatial–temporal localization of E-cadherin was determined in the endometrium during endometrial receptivity period in the mouse model. (**A**) Cellular distribution of E-cadherin in the mouse endometrium during the receptivity period was performed with the help of immunohistochemistry (IHC). (**B**) We determined the cellular distri-bution of E-cadherin in the endometrium during lipopolysaccharide (LPS)-induced implantation mouse model using IHC. The scale bar in Fig. 2A are 60 μm and 30 μm for the objective lens 20× and 40×, respectively. The scale bar in Fig. 2B are 120 μm, 60 μm, and 30 μm for the objective lens 10×, 20×, and 40×, respectively. (*N*=2)
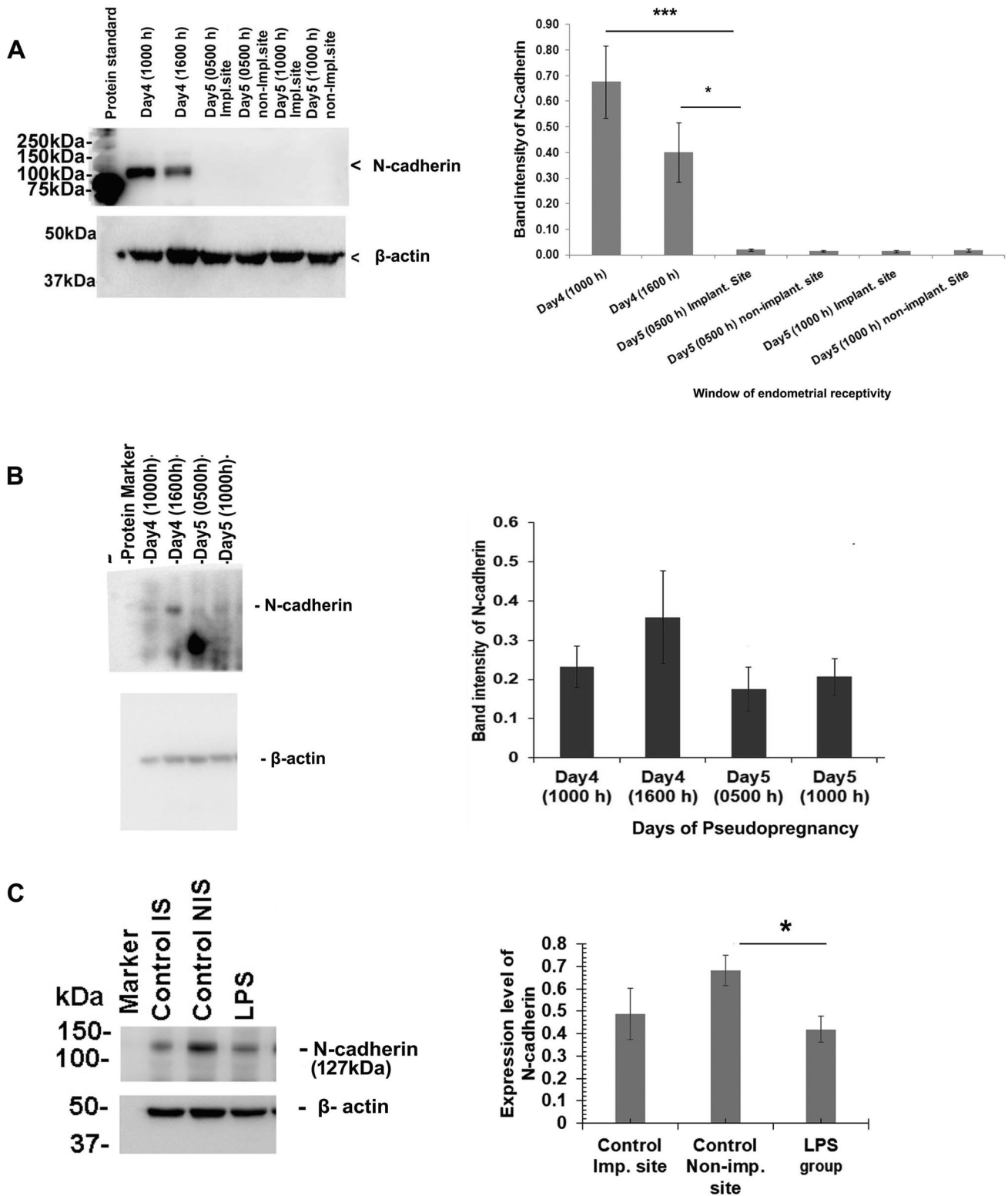
Fig. 3 N-cadherin expression was determined in the endometrium during the receptivity period of mouse model. (**A–C**) Expression profiling of N-cadherin was performed with the help of immunoblotting and densitometric analysis in the uterus during the normal receptivity period, pseudopregnancy/receptivity and LPS-induced failed receptivity for the blastocyst implantation. ($N=4$) (***$p < 0.0005$, *$p < 0.05$, NS $p > 0.05$)

receptivity stages and decreased during day 5, 0500 h stage implantation region, and was not detectable at the subsequent stage (day 5, 1000 h) (Fig. 3A). During pseudopregnancy in mouse model, N-cadherin was present in the endometrium throughout the studied stages of window of endometrial receptivity and was found higher at the pre-implantation stages (day 4, 1000 h and 1600 h) (Fig. 3B), decreasing during subsequent stages, receptive and post-receptive (day 5, 0500 and 1000 h); the expression level of N-cadherin was decreased (Fig. 3B); though, there was no statistical significance difference among the stages studied (Fig. 3B).

Further, using LPS-induced blastocyst implantation failure model, we examined N-cadherin association with endometrial receptivity. Unlike E-cadherin, N-cadherin showed a reverse pattern, where it was found decreased at the control implantation sites and increased at the non-implantation sites in the normal implantation group at day 5, 1000 h (Fig. 3C). In the LPS-induced implantation failure mouse model, the expression of N-cadherin was downregulated in comparison to the normal implantation non-implantation site (Fig. 3C), but remained nearly same to the control implantation site.

Furthermore, we examined the cellular distribution pattern of the N-cadherin in the endometrium during the window of endometrial receptivity period and LPS-induced implantation failure mouse model (Fig. 4A and B). The expression of N-cadherin was seen in the epithelial (luminal and glandular) and stromal cells during the pre-receptive stage (day 4, 1000 h). The following stage (day 4, 1600 h) showed the expression of N-cadherin in the glandular and luminal epithelial cells (Fig. 4A). The next stage of endometrial receptivity receptive stage (day 5, 0500 h) showed N-cadherin expression in the endometrial stromal and luminal epithelial cells, but not detectable in the glandular epithelial cells. Subsequently, post-receptive stage (day 5, 1000 h) showed expression of N-cadherin in stromal cells and mild expression in the epithelial cells (luminal and glandular) (Fig. 4A). The immunolabelling with normal rabbit IgG on the uterine tissue did not show significant staining, suggesting the anti-N-cadherin rabbit IgG specific immunostaining (Fig. 2A).

Subsequently, we determined the expression level of N-cadherin in the endometrium from the normal embryo implantation and LPS-treated group of animals (Fig. 4B). The normal implantation and LPS-induced implantation failure groups showed the expression of N-cadherin in the endometrial stromal and luminal epithelial cells and not detectable in the glandular epithelial cells at day 5 (1000 h p.c.). The observed expression pattern of N-cadherin in the normal embryo implantation group without the LPS treatment was not different from the LPS-treated group

(Fig. 4B). Further, there is no distinguishable expression of N-cadherin in the implantation and non-implantation regions.

E-cadherin Regulator, GSK-3, Expression was Downregulated and Suppressor, SLUG, was Upregulated During Receptive Stage of Endometrium

Glycogen synthase kinase (GSK)-3 is a known E-cadherin promoter, and here, we studied its expression during window of endometrial receptivity stages. GSK-3 expression was detected during the endometrial receptivity stages, and we found high expression level during pre-receptive stage (day 4, 1000 h), declined during the subsequent, late-pre-receptive (day 4, 1600 h) and receptive (day 5, 0500 h) stages at both implantation and non-implantation sites (Fig. 5A). The expression level of GSK-3 was regained high at post-receptive stage (day 5, 1000 h) implantation and non-implantation regions (Fig. 5A).

Later, we examined the expression level of GSK-3 in the LPS-induced embryo implantation mouse model (Fig. 5B). The expression level of GSK-3 was in moderate levels in the control (normal) embryo implantation group implantation and non-implantation regions, but increased in the LPS-induced implantation failure group, and it was statistically non-significant (Fig. 5B).

In contrast, the expression levels of the expression of E-cadherin suppressor SLUG was low during the pre-receptive stage, but subsequently increased with the higher expression on receptive stage (day 5, 0500 h) at both the implantation and non-implantation sites (Fig. 5C). The following advance stage, post-receptive stage, SLUG expression was reduced at both implantation and non-implantation sites (Fig. 5C).

PARP-2 Promotes E-cadherin (Phosphorylation) in the Human Endometrial Epithelial Cells (hEECs)

PARP-1 can regulate the E-cadherin expression in non-endometrial cells [12]. Therefore, we explored the regulation of E-cadherin and in emphasis to PARP-2 signaling dependent in the hEECs after the PARP-2 pharmacological inhibition. We found that PARP-2 activity promoted the expression of phosphorylated E-cadherin, but the expression of N-cadherin was suppressed (Fig. 6A and B). However, caspase-8, a critical regulator of PARP-2 in mouse endometrial receptivity [15], inhibition had no effect on the E-cadherin and N-cadherin expression (Fig. 6C and D).
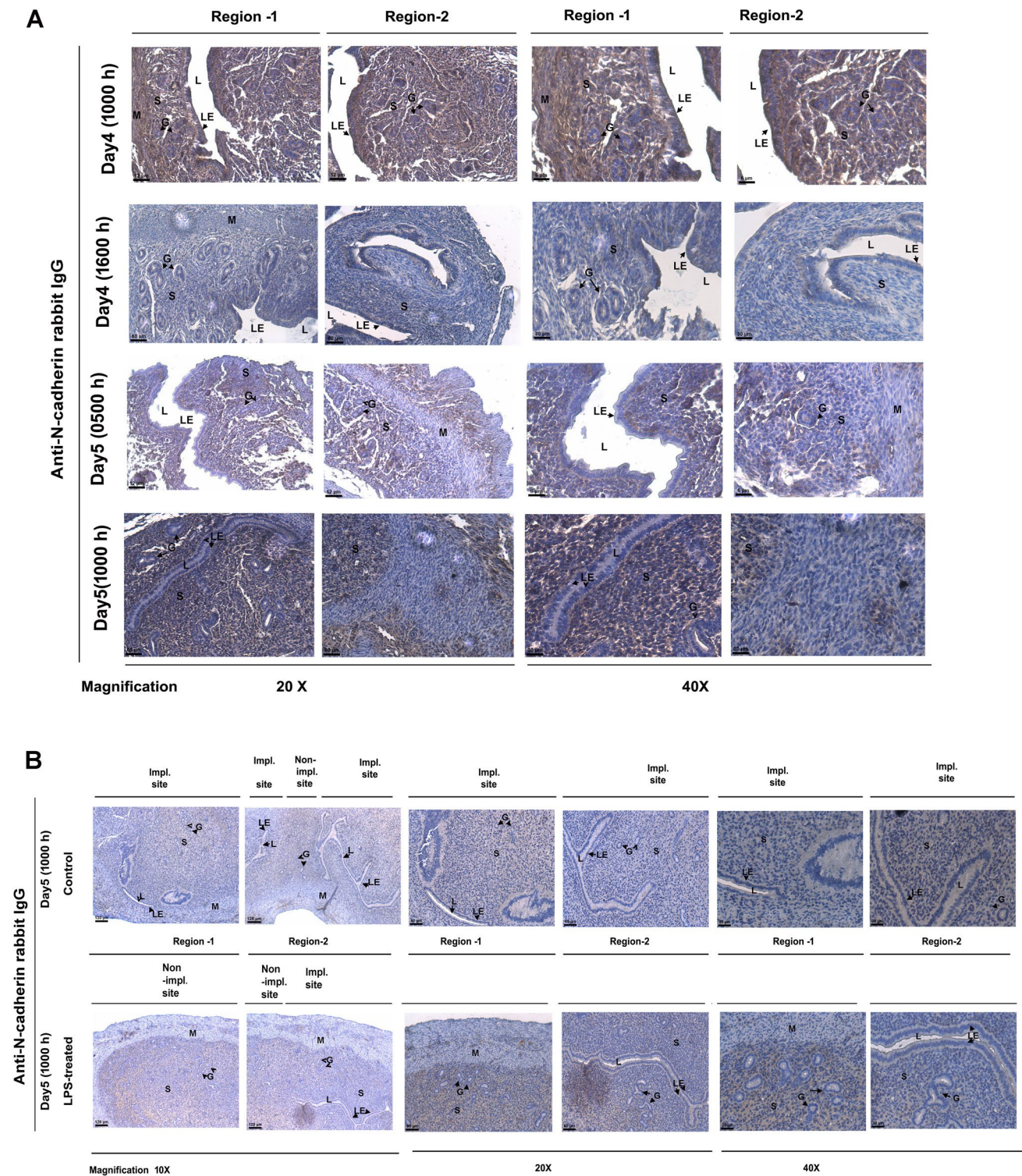
Fig. 4 Spatiotemporal localization of N-cadherin was examined in the mouse endometrium during endometrial receptivity period. (**A**) We performed the cellular distribution analysis of N-cadherin in the endometrium during the receptivity period with the help of IHC. (**B**) Using IHC, the cellular localization of N-cadherin was done in the endometrium from LPS-induced implantation mouse model. The scale bar in Fig. 2A are 60 μm and 30 μm for the objective lens 20× and 40×, respectively. The scale bar in Fig. 2B are 120 μm, 60 μm, and 30 μm for the objective lens 10×, 20×, and 40×, respectively
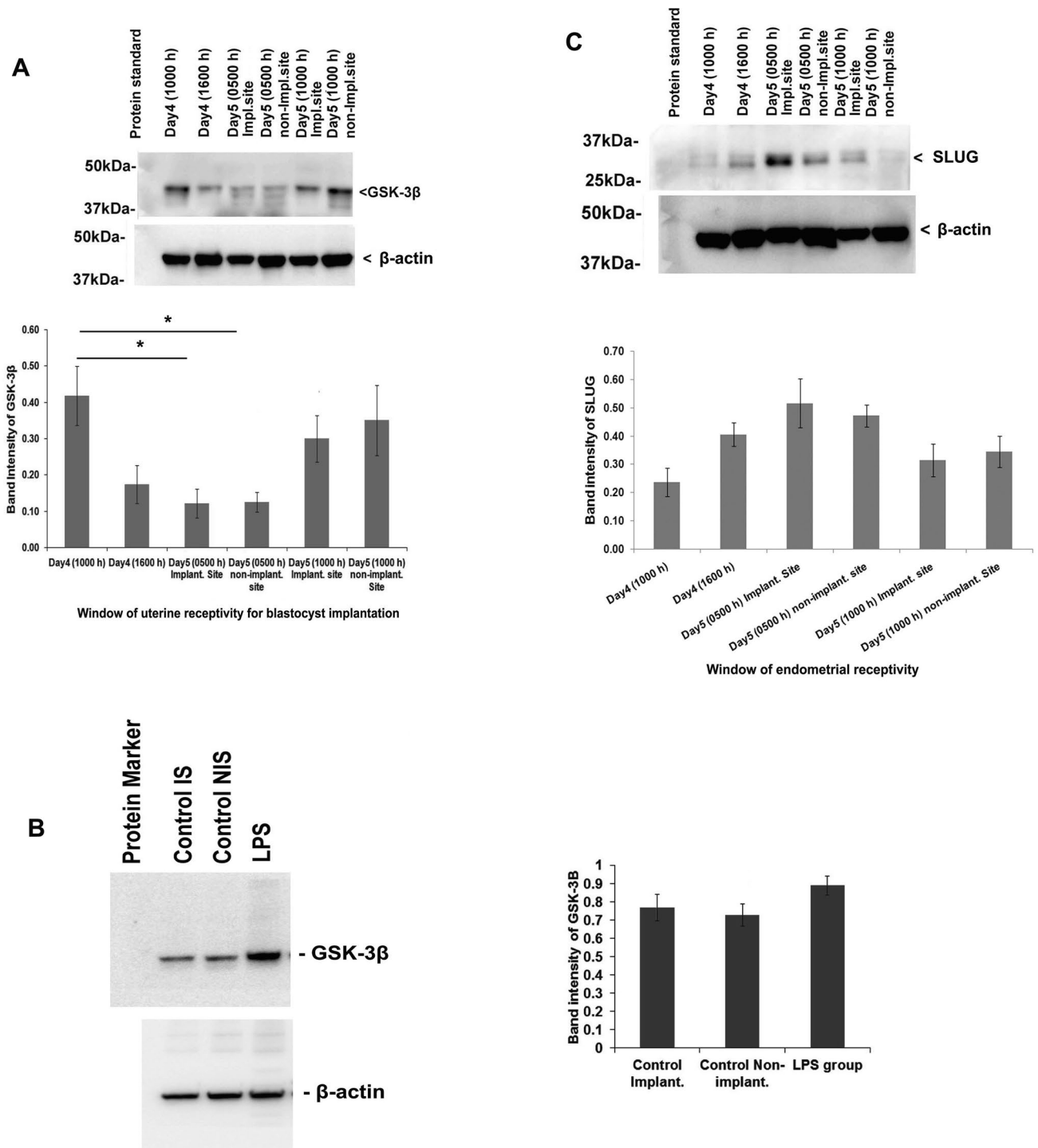
Fig. 5 E-cadherin and N-cadherin regulatory signaling molecules, GSK-3 and SLUG are differentially expressed during endometrial receptivity in the mouse model. (**A**) and (**B**) Expression profiling of glycogen synthase kinase (GSK)-3 was performed with the help of immunoblotting and densitometric analysis in the mouse uterus dur-ing the normal receptivity for the blastocyst implantation and LPS-induced embryo implantation failure. (**C**) The differential expression analysis of SLUG was done with the help of immunoblotting and densitometric analysis in the mouse uterus during the receptivity/implantation period. ($N=4$) (NS, $p>0.05$, *$p<0.05$)

PARP-2 Is Localized in the Stromal Regions of Implantation Sites at Post-Receptive Stages, Day 5 (1000 h)

While PARP-2 localization in the endometrial cells is already established [15], we observed PARP-2 localization in the stromal and epithelial cells (luminal and glandular).
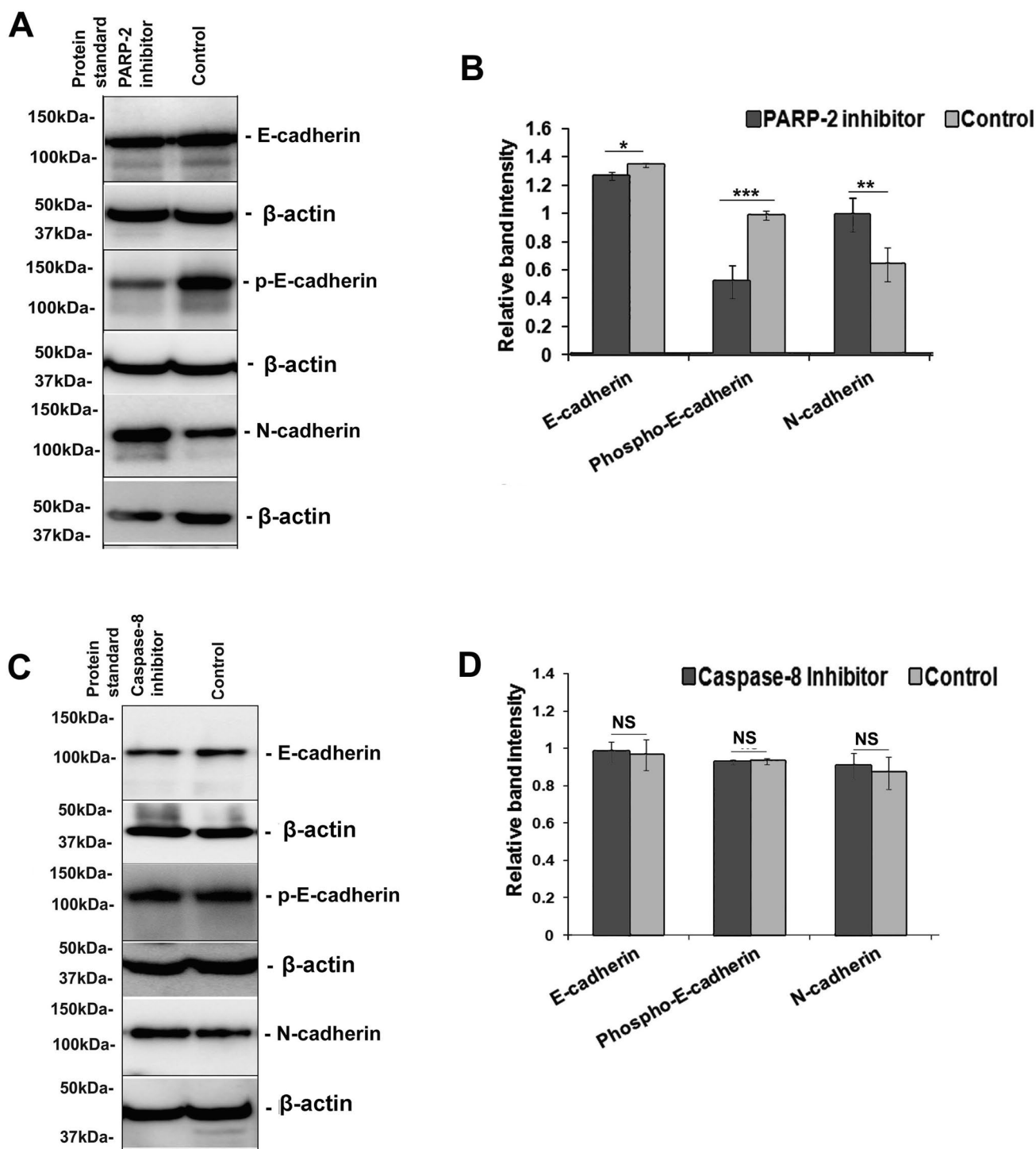
Fig. 6 E-cadherin expression is promoted by PARP-2 in the human endometrial epithelial cells (hEECs). (**A–B**) E-cadherin, phosphorylated-E-cadherin, and N-cadherin expression in the hEECs in response to PARP-2 pharmacological inhibition was analyzed by immunoblotting and densitometric analysis. (**C–D**) E-cadherin, phosphorylated-E-cadherin, and N-cadherin expression in the hEECs in response to caspase-8 pharmacological inhibition was determined by immunoblotting and densitometric analysis. ($N = 3$) ($***p < 0.005$, $**p < 0.005$, $*p < 0.05$, NS $p > 0.05$)

We localized PARP-2 to know the cellular distribution in the pregnant endometrium. By employing immunohistochemistry in longitudinal uterine sections comprised of

implantation and non-implantation sites during day 5, 1000 h stage, we performed the immunolocalization of PARP-2. We histologically confirmed the presence of implantation and
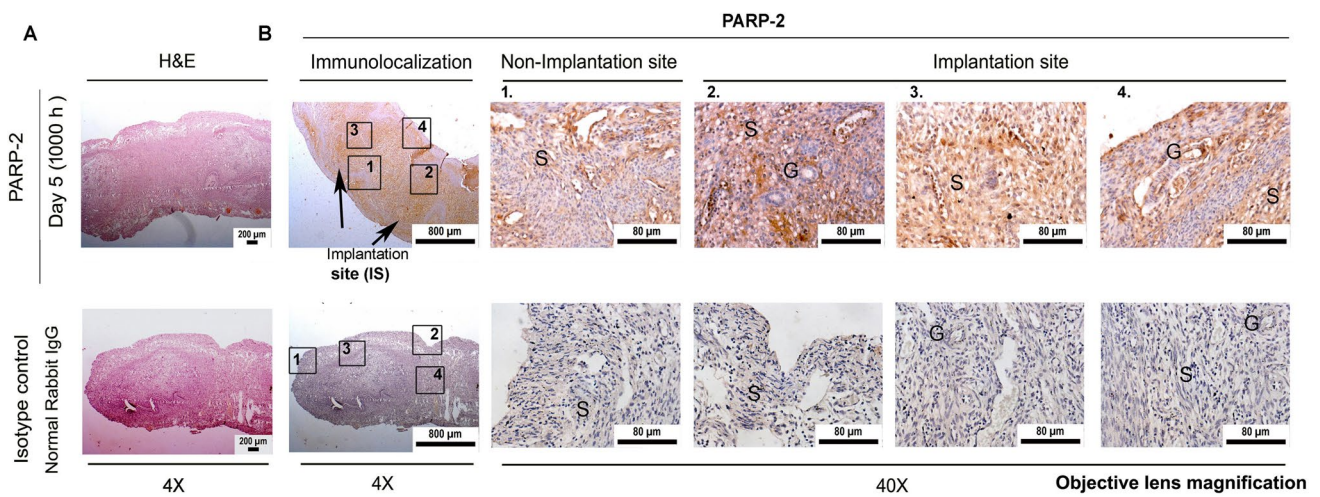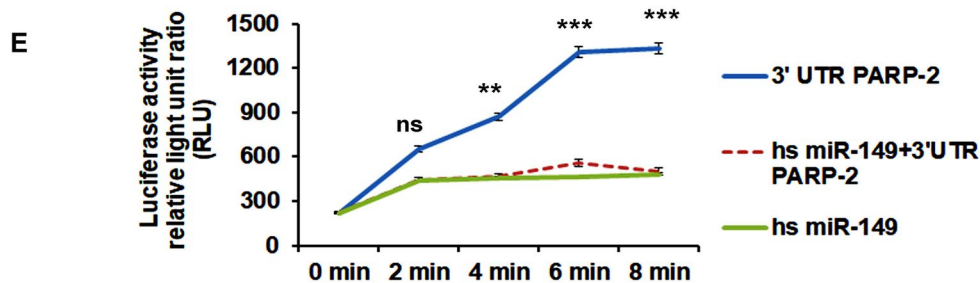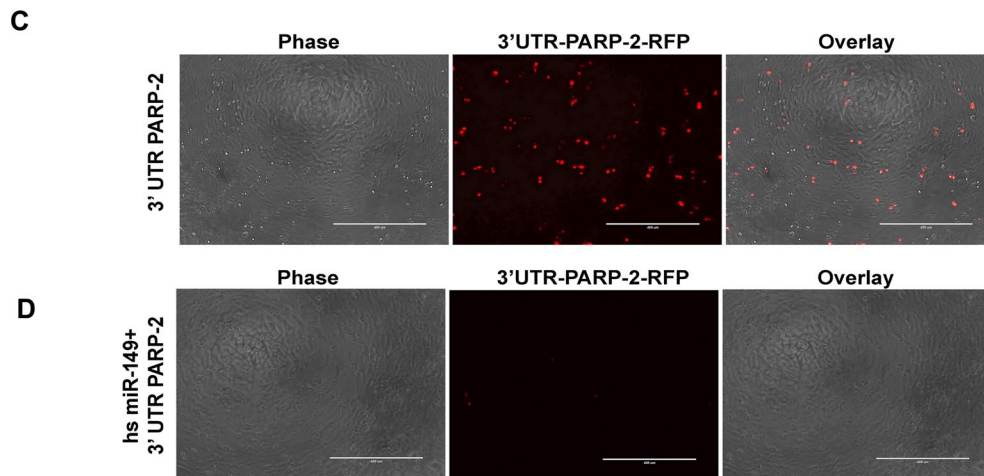
Fig. 7 Uterine-PARP-2 spatial–temporal localization and miR-149 binding with PARP-2 3′UTR were examined. (**A-B**) We performed the cellular distribution analysis of poly(ADP-ribose) polymerase (PARP)-2 in the longitudinal sections of endometrium (uterus) during the receptivity period with the help of IHC and H&E. (**C–D**) hEECs were transfected with 3′UTR PARP-2 red fluorescence protein (RFP) and hs-miR-149 + 3′UTR PARP-2-RFP plasmids and imaged after the 48 h of transfection. (**E**) After the transfection, the luciferase activity in relative light unit ratio (RLU) was analyzed. ($N=3$) (***$p<0.005$, **$p<0.005$, NS $p>0.05$). The scale bar in Fig. 7A is 200 μm for the objective lens 4×. The scale bar in Fig. 7B are 800 μm and 80 μm for the objective lens 4× and 40×, respectively

A

Transfection in hEECS for 48 hours

E-cadherin/ Control plasmid-Non-GFP/ DAPI

63X · 0 µm 100 · 126X · 0 µm 50

B

E-cadherin/ Hs miR-149-Turbo-GFP/ DAPI

63X · 0 µm 100 · 126X · 0 µm 50

C

(-Ve control) Hs miR-149-Turbo-GFP/ DAPI

63X · 0 µm 100 · 126X · 0 µm 50

D

E

Co-culture of JEG-3 spheroids with hEECs monolayer

E-cad / miR-149-GFP / DAPI

E-cad / Control vector-Non-GFP / DAPI

63 X · hEECs monolayer · JEG-3 spheroid · 0 µm 100

189 X · 0 µm 50

F

Protein marker (kDa): 250, 150, 100, 75, 50, 37

- miR-149, - Control plasmid

- E-cadherin
- β-actin

Relative expression levels of E-cadherin ***

Ishikawa cells: miR-149 plasmid, Control plasmid

G

Protein marker (kDa): 150, 100, 75, 50, 37

- miR-149, - Control plasmid

- N-cadherin
- β-actin

Relative expression level of N-cadherin NS

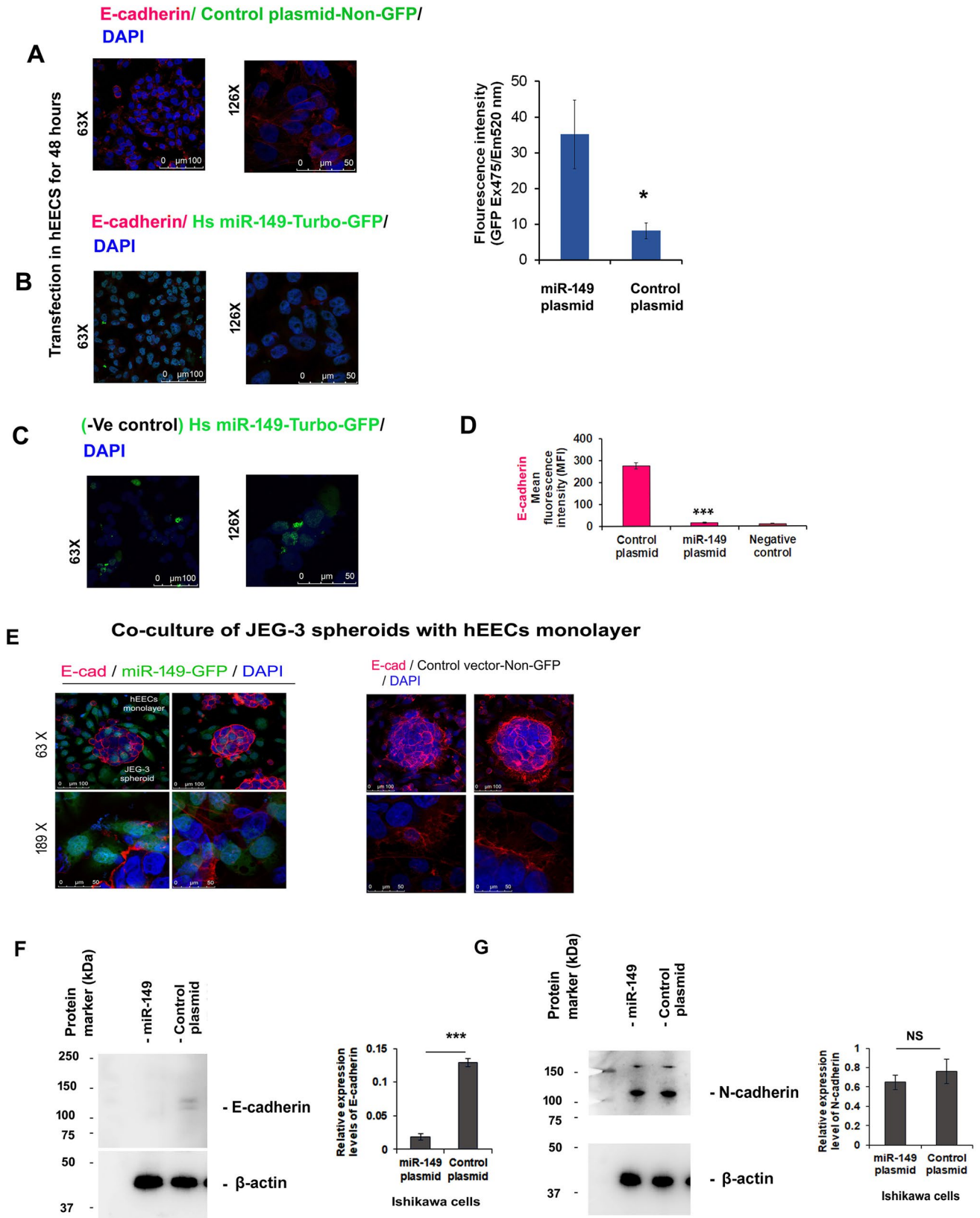Ishikawa cells: miR-149 plasmid, Control plasmid

◄**Fig. 8** E-cadherin expression is regulated by miR-149 in the hEECs. E-cadherin fluorescence in (**A**) control plasmid (**B**) miR-149 plasmid transfected hEECs was imaged by confocal laser scanning microscopy. (**C**) A negative control for E-cadherin (red) was performed and imaged by confocal laser scanning microscopy in the miR-149 green fluorescence protein (GFP) plasmid transfected endometrial epithelial cells. (**D**) E-cadherin fluorescence intensity was determined by confocal laser scanning microscopy imaging software. (**E**) Localization of E-cadherin was performed with the help of immunofluorescence in the hEECs and human trophoblast cells (hTBLC) 3D spheroids in response to miR-149 overexpression. (**F**–**G**) E-cadherin and N-cadherin expression analysis were done in the human endometrial epithelial cells (hEECs) after miR-149 transfection using immunoblotting and densitometry. ($N=3$) (***$p<0.005$, NS $p>0.05$). The scale bar in Fig. 8A, B, and E and are 100 μm and 50 μm for the objective lens 63× and 126×/189×, respectively

non-implantation regions from day 5 (1000 h) p.c. uterus (Fig. 7A). We observed the cellular distribution of PARP-2 in the endometrial stromal and epithelial (luminal and glandular) at day 5 (1000 h) p.c. (Fig. 7B and C). The immuno-labelling with the normal rabbit IgG, as an isotype control, showed no significant DAB signal, confirming the PARP-2 antibody-specific immunostaining (Fig. 7B lower panel).

miR-149 Regulates E-cadherin Expression via PARP-2

Earlier findings indicate that PARP-2 is directly regulated by miR-149 [16], and we have also recently shown that miR-149 regulates PARP-2 expression in hEECs and human endometrial stromal cells (T-hESCs) [14]. We reconfirmed that miR-149 binds with PARP-2 3′UTR. A reporter was constructed containing the luciferase gene fused to the PARP-2 3′-UTR (luc-PARP–3′-UTR), which was then transfected into human endometrial epithelial cells with or without a miR-149 overexpression vector. Cells transfected with luc-PARP-2 3′-UTR alone had luciferase activity, while cells co-transfected with pEGP-miR-149 displayed significantly reduced luciferase activity, providing experimental evidence that PARP-2 is a direct target gene of miR-149 (Fig. 7C–E).

Subsequently, the expression of E-cadherin was assessed in human endometrial epithelial cells transfected with miR149-GFP (green) or control vector. Overexpression of miR149-GFP, as confirmed by the green fluorescence, inhibited E-cadherin expression (shown in red) compared to control cells (Fig. 8A, B, and D). The rabbit IgG tetramethylrhodamine (TRITC) served as a negative control for E-cadherin staining with no detectable fluorescence intensity (Fig. 8C and D). Subsequently, we examined the expression of E-cadherin in hEECs and hTBLC 3D spheroids with the help of immunofluorescence. E-cadherin was present at the interface of attached hTBLC spheroids and hEECs in the control condition (Fig. 8E): E-cadherin was present in both cell types (red) (Fig. 8E).

Furthermore, we performed immunoblotting analysis post-miR-149 or control plasmids overexpression in the hEECs. The expression level of E-cadherin was fairly detected in response to control plasmid and downregulated in response to miR-149 overexpression (Fig. 8F). In contrast, the expression of N-cadherin remained unaltered in the overexpression of miR-149 in the hEECs (Fig. 8G).

In summary, our findings show differential expression of the cadherins and their modulators during the endometrial receptivity window in the mouse and a role for miR-149 controls of E-cadherin expression via PARP-2 in the hEECs, Ishikawa.

Discussion

Herein, we report that E-cadherin and N-cadherin downregulate during receptive states of window of endometrial receptivity and miR-149 regulates E-cadherin via PARP-2 in the endometrial epithelial cell, which demonstrated new signaling of E-cadherin regulation in the endometrial cells.

Previously, E-cadherin and N-cadherin were shown associated with endometrial receptivity where E-cadherin upregulation in the human endometrial epithelial cells (hEECs) favors the receptivity [4] linked with EMT events [5]. Earlier reports suggested that loss of E-cadherin is essential for endometrial receptivity [9, 28]. However, our previous work has demonstrated the presence of E-cadherin in the endometrium during these stages [3]. Nonetheless, no observation was made on the phosphorylated form of E-cadherin and N-cadherin during endometrial receptivity. We set out to investigate the changes in these cadherins between implantation regions and epigenetic regulation by miR-149-PARP-2 signaling and show higher levels of E-cadherin and its phosphorylated form during early receptive stage that are maintained during late-pre-receptive stage. The expression of E-cadherin was decreased in the implantation region of our model during the receptive stage from normal pregnancy. Furthermore, downregulation of E-cadherin was observed in the receptive stage of pseudopregnancy, suggesting that downregulation of E-cadherin may facilitate loss of the polarity in the endometrial cells as reported [9].

We observed the localization of E-cadherin ubiquitously in the endometrial cells during pre-receptive stage, which showed restricted expression in the epithelial cells (glandular and luminal region) at late-pre-receptive stage and changed to stromal region during the receptive and post-receptive stages, suggesting downregulation of E-cadherin to facilitate the loss of the cells polarity in the endometrial cells, as reported previously [9]. The LPS-induced implantation failure showed upregulation of E-cadherin then the normal implantation, indicating dysregulation of E-cadherin expression in the endometrium.

EMT is an integral part of the endometrial receptivity [5], and N-cadherin is one of the biomarkers for this process. In fact, alteration of N-cadherin has been implicated in infertility [11]. In our experiments, expression was downregulated in the pregnancy failure cases. Interestingly, we observed expression of N-cadherin during pre-receptive and late-pre-receptive stages followed by decrease in expression at receptive and post-receptive stages of normal and pseudopregnancies in mouse model, suggesting downregulation of N-cadherin once the endometrial receptivity is achieved. Further, N-cadherin expression was negatively affected by the LPS-induced embryo implantation failure in the mouse model.

Collectively, E-cadherin and N-cadherin expressions were decreased at the receptive and post-receptive stages of normal- and pseudo-pregnancies, indicating the implantation stage specific downregulation of E-cadherin and N-cadherin in the uterus. The cellular distribution of E-cadherin was epithelial (luminal and glandular) and stromal cells during the day 4 (100 h and 1600 h) stages, which became prominent on the luminal and glandular epithelial cells, but reduced at day 5, 1000 h. N-cadherin cellular distribution was seen epithelial (luminal and glandular) and stromal cells during the pre-receptive phase (day 4, 1000 h) and reduced from stromal cells at day 4, 1600 h. The receptive stage, day 5, 0500 h, E-cadherin was reduced in the glandular epithelial cells. At the advanced stage, day 5, 1000 h, N-cadherin localization was strong on the stromal cells and mild on the epithelial cells (luminal and glandular).

To confirm the role of E-cadherin and N-cadherin in the endometrial receptivity, we utilized a LPS-induced endometrial receptivity failure model and found that on the post-receptive (day 5, 1000 h) stage of pregnancy, post-LPS-administration, N-cadherin was decreased at the LPS-induced endometrial receptivity failure as well as normal pregnancy/receptivity implantation sites, indicating its requirement for endometrial receptivity preparation. However, E-cadherin expression was lower in the implantation site of normal endometrial receptivity compared to non-implantation sites, and LPS administration showed similar expression of E-cadherin to non-implantation sites of normal endometrial receptivity, suggesting downregulation of E-cadherin expression is necessary for endometrial receptivity. At the cellular level, E-cadherin was prominent in the stromal and luminal epithelial cells and mildly in the glandular epithelial cells at day 5 (1000 h p.c.) of normal embryo implantation and LPS-induced embryo failures groups. The expression of N-cadherin was seen in the endometrial stromal and luminal epithelial cells and not detectable in the glandular epithelial cells at day 5(1000 h p.c.) of either normal implantation or LPS-induced implantation failure groups. However, further studies are required to delineate

the role of E-cadherin and N-cadherin in a cell-specific manner during the endometrial receptivity.

Another EMT biomarker, a member of the SNAIL family of transcriptional repressors, SLUG, [29] was increased in the implantation site during the receptive stage, indicating a EMT like event. In contrast GSK-3, an E-cadherin promoter [30], was downregulated during the receptive stage at both implantation and non-implantation sites of the endometrium, but its expression was seen during pre-receptive and post-receptive stages predominantly. The LPS-induced implantation failure model increased the expression level of GSK-3 in the endometrium. Overall, our experiments support an EMT-like phenomenon in a receptive uterus involving SLUG, with the downregulation of E-cadherin, N-cadherin, and GSK-3β. Nonetheless, further investigations are required to validate it. It has been found that LPS induces inflammation by upregulation of TNF-α, IL-1, and IL-6 cytokines and miR-149 can suppress in the nucleus pulposus cells [31]. Likewise, the possibility could be there in the uterine receptivity failure by LPS administration, and miR-149 might influence it, but the mechanism is yet to be established.

Subsequently, we explored the regulation of E-cadherin and N-cadherin in hEECs. Pharmacological inhibition of PARP-2 in the hEECs showed downregulation in the expression level of E-cadherin and its phosphorylated forms. Interestingly, expression of N-cadherin was increased, indicating PARP-2-dependent differential regulation of E-cadherin and N-cadherin in the hEECs. Inhibition of caspase-8, a regulator of PARP-2, did not affect either of the studied cadherins, suggesting a possible redundancy of caspase-8 in the cadherins' regulatory pathway. However, further studies are needed to further confirm the caspase-8 signaling in this context.

PARP-2 is post-transcriptionally regulated by miR-149 as this particular miRNA binds to the 3'UTR of PARP-2 [16]. Further, we recently found that miR-149 regulates PARP-2 expression in the hEECs and T-hESCs rendering poor trophoblast attachment [14] and miR-149 has been reported to downregulate the E-cadherin expression [32]. PARPs in cancerous cells [33, 34] showed E-cadherin downregulation, indicating some regulatory mechanism. Therefore, we analyzed the miR-149-PARP-2-dependent E-cadherin and N-cadherin expression regulation in hEECs. We confirmed that miR-149 downregulates E-cadherin expression, but does not affect the N-cadherin expression, which corroborates our earlier observation in the mouse model of endometrial receptivity where the downregulated miR-149 and upregulated PARP-2 facilitates the endometrial receptivity for embryo implantation [14, 15]. The study is based on the human endometrial epithelial cancerous cells (Ishikawa) based data; hence, interpretation needs to be carefully made. Our findings provide evidence that miR-149, via PARP-2, controls E-cadherin expression in endometrial epithelial cells.

Conclusion

In conclusion, the loss of E-cadherin and N-cadherin was observed during acquisition of endometrial receptivity (normal and pseudopregnancy). Further, we revealed that E-cadherin is upregulated in the LPS-induced endometrial receptivity failure mouse model. Finally, we demonstrated that miR-149-PARP-2 signaling regulates E-cadherin expression in the human endometrial epithelial cells, Ishikawa.

Author Contribution RKV contributed in Figs. 1C, D and E, 2A and B, 3B and C, and 5B. UKS contributed in Figs. 7 and 8. SBC contributed to Figs. 3A, 5A and C, and 6A, B, C, and D. VKM contributed to Fig. 1A–B. MS contributed to Fig. 7C and D. SS contributed in Fig. 4A and B. JVP contributed to the Fig. 7C and D conceptualization. RKJ conceptualized the overall study design, analyzed the data, and wrote the manuscript.

Data availability The authors state that data are available upon request from the corresponding author.

Code availability No applicable.

Declarations

Ethics approval Animal handling and care were done according to the Animal Ethical Committee Guidelines of CSIR-Central Drug Research Institute (CDRI), Lucknow, India, and this study was approved via application file nos. IAEC/2013/27 dated 7.3.2013 and IAEC/2019/39/ dated 04/01/2019.

Consent to participate Not applicable.

Consent for publication The consent stands for the publication.

Conflict of interest The authors declare no competing interests.

References

1. Bellati F, Costanzi F, De Marco MP, Cippitelli C, Stoppacciaro A, De Angelis C, Ruscito I, Rago R, Caserta D. Low endometrial beta-catenin and cadherins expression patterns are predictive for primary infertility and recurrent pregnancy loss. Gynecol Endocrinol. 2019;35:727–31.

2. Lopes IM, Maganhin CC, Oliveira-Filho RM, Simoes RS, Simoes MJ, Iwata MC, Baracat EC, Soares JM Jr. Histomorphometric Analysis and markers of endometrial receptivity embryonic implantation in women with polycystic ovary syndrome during the treatment with progesterone. Reprod Sci. 2014;21:930–8.

3. Jha RK, Titus S, Saxena D, Kumar PG, Laloraya M. Profiling of E-cadherin, beta-catenin and Ca(2+) in embryo-uterine interactions at implantation. FEBS Lett. 2006;580:5653–60.

4. Rahnama F, Thompson B, Steiner M, Shafiei F, Lobie PE, Mitchell MD. Epigenetic regulation of E-cadherin controls endometrial receptivity. Endocrinology. 2009;150:1466–72.

5. Kononistov Iu I, Borodulin BP. Bilateral acute suppurative pyelonephritis in pregnancy complicated by acute renal failure. Akush Ginekol (Mosk). 1988: Jun (6): 62.

6. Bartley J, Julicher A, Hotz B, Mechsner S, Hotz H. Epithelial to mesenchymal transition (EMT) seems to be regulated differently in endometriosis and the endometrium. Arch Gynecol Obstet. 2014;289:871–81.

7. Gou J, Hu T, Li L, Xue L, Zhao X, Yi T, Li Z. Role of epithelial-mesenchymal transition regulated by twist basic helix-loop-helix transcription factor 2 (Twist2) in embryo implantation in mice. Reprod Fertil Dev. 2019;31:932–40.

8. Shirane A, Wada-Hiraike O, Tanikawa M, Seiki T, Hiraike H, Miyamoto Y, Sone K, Hirano M, Oishi H, Oda K, Kawana K, Nakagawa S, Osuga Y, Fujii T, Yano T, Kozuma S, Taketani Y. Regulation of SIRT1 determines initial step of endometrial receptivity by controlling E-cadherin expression. Biochem Biophys Res Commun. 2012;424:604–10.

9. Liang J, Cao D, Zhang X, Liu L, Tan Q, Shi S, Chen K, Liang J, Wang Z. miR-192-5p suppresses uterine receptivity formation through impeding epithelial transformation during embryo implantation. Theriogenology. 2020;157:360–71.

10. Revel A, Achache H, Stevens J, Smith Y, Reich R. MicroRNAs are associated with human embryo implantation defects. Hum Reprod. 2011;26:2830–40.

11. Makker A, Goel MM, Nigam D, Bhatia V, Mahdi AA, Das V, Pandey A. Endometrial expression of homeobox genes and cell adhesion molecules in infertile women with intramural fibroids during window of implantation. Reprod Sci. 2017;24:435–44.

12. McPhee TR, McDonald PC, Oloumi A, Dedhar S. Integrin-linked kinase regulates E-cadherin expression through PARP-1. Dev Dyn. 2008;237:2737–47.

13. Joshi A, Mahfooz S, Maurya VK, Kumar V, Basanna CS, Kaur G, Hanif K, Jha RK. PARP1 during embryo implantation and its upregulation by oestradiol in mice. Reproduction. 2014;147:765–80.

14. Soni UK, Chadchan SB, Gupta RK, Kumar V, Jha RK. miRNA-149 targets PARP-2 in endometrial epithelial and stromalcells to regulate the trophoblast attachment process. Mol Hum Reprod. 2021;27(6):gaab039.

15. Soni UK, Chadchan SB, Joshi A, Kumar V, Maurya VK, Verma RK, Jha RK. Poly(ADP-ribose) polymerase-2 is essential for endometrial receptivity and blastocyst implantation, and regulated by caspase-8. Mol Cell Endocrinol. 2020;518:110946.

16. Mohamed JS, Hajira A, Pardo PS, Boriek AM. MicroRNA-149 inhibits PARP-2 and promotes mitochondrial biogenesis via SIRT-1/PGC-1alpha network in skeletal muscle. Diabetes. 2014;63:1546–59.

17. Chadchan SB, Kumar V, Maurya VK, Soni UK, Jha RK. Endoglin (CD105) coordinates the process of endometrial receptivity for embryo implantation. Mol Cell Endocrinol. 2016;425:69–83.

18. Kondoh E, Okamoto T, Higuchi T, Tatsumi K, Baba T, Murphy SK, Takakura K, Konishi I, Fujii S. Stress affects uterine receptivity through an ovarian-independent pathway. Hum Reprod. 2009;24:945–53.

19. Yu M, Cui X, Wang H, Liu J, Qin H, Liu S, Yan Q. FUT8 drives the proliferation and invasion of trophoblastic cells via IGF-1/IGF-1R signaling pathway. Placenta. 2019;75:45–53.

20. Vergaro P, Tiscornia G, Rodriguez A, Santalo J, Vassena R. Transcriptomic analysis of the interaction of choriocarcinoma spheroids with receptive vs. non-receptive endometrial epithelium cell lines: an in vitro model for human implantation. J Assist Reprod Genet. 2019;36:857–73.

21. Li Q, Chiu PCN, Yeung WSB, Liu W. Regulation of human trophoblast surrogate Jeg-3 spheroids implantation potential by Wnt/beta-catenin pathway and lin28a/let-7a axis. Exp Cell Res. 2020;388:111718.

22. Elbaz M, Hadas R, Bilezikjian LM, Gershon E. Uterine Foxl2 regulates the adherence of the trophectoderm cells to the endometrial epithelium. Reprod Biol Endocrinol. 2018;16:12.

23. Kumar V, Soni UK, Maurya VK, Singh K, Jha RK. Integrin beta8 (ITGB8) activates VAV-RAC1 signaling via FAK in the acquisition of endometrial epithelial cell receptivity for blastocyst implantation. Sci Rep. 2017;7:1885.

24. Kumar V, Maurya VK, Joshi A, Meeran SM, Jha RK. Integrin beta 8 (ITGB8) regulates embryo implantation potentially via controlling the activity of TGF-B1 in mice. Biol Reprod. 2015;92:109.

25. Ubba V, Soni UK, Chadchan S, Maurya VK, Kumar V, Maurya R, Chaturvedi H, Singh R, Dwivedi A, Jha RK. RHOG-DOCK1-RAC1 signaling axis is perturbed in DHEA-induced polycystic ovary in rat model. Reprod Sci. 2017;24:738–52.

26. Davoodi-Semiromi A, Laloraya M, Kumar GP, Purohit S, Jha RK, She JX. A mutant Stat5b with weaker DNA binding affinity defines a key defective pathway in nonobese diabetic mice. J Biol Chem. 2004;279:11553–61.

27. Towbin H, Staehelin T, Gordon J. Electrophoretic transfer of proteins from polyacrylamide gels to nitrocellulose sheets: procedure and some applications. 1979. Biotechnology. 1992;24:145–9.

28. Yang Y, Chen X, Saravelos SH, Liu Y, Huang J, Zhang J, Li TC. HOXA-10 and E-cadherin expression in the endometrium of women with recurrent implantation failure and recurrent miscarriage. Fertil Steril. 2017;107(136–143).

29. Phillips S, Kuperwasser C. SLUG: critical regulator of epithelial cell identity in breast development and cancer. Cell Adh Migr. 2014;8:578–87.

30. Doble BW, Woodgett JR. Role of glycogen synthase kinase-3 in cell fate and epithelial-mesenchymal transitions. Cells Tissues Organs. 2007;185:73–84.

31. Qin C, Lv Y, Zhao H, Yang B, Zhang P. MicroRNA-149 suppresses inflammation in nucleus pulposus cells of intervertebral discs by regulating MyD88. Med Sci Monit. 2019;25:4892–900.

32. Luo Z, Zhang L, Li Z, Jiang C, Dai Y, Liu X, Zheng Y, Yu H, Xiang J, Li G. miR-149 promotes epithelial-mesenchymal transition and invasion in nasopharyngeal carcinoma cells. Zhong Nan Da Xue Xue Bao Yi Xue Ban. 2011;36:604–9.

33. Rodriguez MI, Gonzalez-Flores A, Dantzer F, Collard J, de Herreros AG, Oliver FJ. Poly(ADP-ribose)-dependent regulation of Snail1 protein stability. Oncogene. 2011;30:4365–72.

34. Kumar M, Jaiswal RK, Yadava PK, Singh RP. An assessment of poly (ADP-ribose) polymerase-1 role in normal and cancer cells. BioFactors. 2020;46:894–905.

35. Kopnick AL, Jansen A, Geistlinger K, Epalle NH, Beitz E. Basigin drives intracellular accumulation of l-lactate by harvesting protons and substrate anions. PLoS One. 2021;16:e0249110.

36. Ikonomou L, Herriges MJ, Lewandowski SL, Marsland R 3rd, Villacorta-Martin C, Caballero IS, Frank DB, Sanghrajka RM, Dame K, Kandula MM, Hicks-Berthet J, Lawton ML, Christodoulou C, Fabian AJ, Kolaczyk E, Varelas X, Morrisey EE, Shannon JM, Mehta P, Kotton DN. The in vivo genetic program of murine primordial lung epithelial progenitors. Nat Commun. 2020;11:635.

37. Chen D, Tang P, Wang Y, Wan F, Long J, Zhou J, Zhuang M, Chen X. Downregulation of long non-coding RNA MR4435-2HG suppresses breast cancer progression via the Wnt/beta-catenin signaling pathway. Oncol Lett. 2021;21:373.

38. Wang G, Bai X, Jiang G, Jin S, Wang Q, Wang A, Peng R, Ke A, Bai D. GIT1 overexpression promotes epithelial-mesenchymal transition and predicts poor prognosis in hepatocellular carcinoma. Bioengineered. 2021;12:30–43.

39. Das M, Ellies LG, Kumar D, Sauceda C, Oberg A, Gross E, Mandt T, Newton IG, Kaur M, Sears DD, Webster NJG. Time-restricted feeding normalizes hyperinsulinemia to inhibit breast cancer in obese postmenopausal mouse models. Nat Commun. 2021;12:565.

40. Luff DH, Wojdyla K, Oxley D, Chessa T, Hudson K, Hawkins PT, Stephens LR, Barry ST, Okkenhaug K. PI3Kdelta forms distinct multiprotein complexes at the TCR signalosome in naive and differentiated CD4(+) T cells. Front Immunol. 2021;12:631271.

41. Wang D, Zhang L, Hu A, Wang Y, Liu Y, Yang J, Du N, An X, Wu C, Liu C. Loss of 4.1N in epithelial ovarian cancer results in EMT and matrix-detached cell death resistance. Protein Cell. 2021;12:107–27.

42. Kim CS, Joo SY, Kim IJ, Choi HI, Bae EH, Kim SW, Ma SK. Anti-apoptotic effect of G-protein-coupled receptor 40activation on tumor necrosis factor-alpha-induced injury of rat proximal tubular cells. Int J Mol Sci. 2019;20(14):3386.